Oceanologia

Effect of Meteorological Parameters on Mixed Layer Depth in the Bay of Bengal

--Manuscript Draft--

Manuscript Number:	
Article Type:	Original Article
Keywords:	Mixed layer depth; monsoon; meteorological parameters; seasonal model; Bay of Bengal
Corresponding Author:	Syamsul Rizal Department of Marine Sciences, Faculty of Marine and Fisheries, Universitas Syiah Kuala INDONESIA
First Author:	Muh. Hidayat
Order of Authors:	Muh. Hidayat
	Muhammad Ikhwan
	Reza Wafdan
	Marwan Ramli
	Zainal Muchlisin
	Syamsul Rizal
Abstract:	Monsoon winds exert a significant influence on both atmospheric and oceanic conditions. In the ocean, these winds stir the water column, resulting in a thickened mixed layer and a thermocline layer at deeper depths. This vertical layer is characterized by changes in the temperature of the water column. In this study, we investigated in detail the relationship between five meteorological parameters - air temperature (AirT), specific humidity (SHum), convective precipitation rate (CPrecR), sea level pressure (SLP), and wind stress (TauX and TauY) - and monsoons and mixed layer depth (MLD). Results from the analysis of the seasonal model indicate that the extreme maximum and minimum of the five selected meteorological parameters follow the peaks and troughs of the northeast monsoon (NEM) and southwest monsoon (SWM). In the northern and southern Bay of Bengal (BoB), the MLD followed a seasonal pattern, with almost identical thicknesses in both regions. The study also found that during the winter monsoon months (November-February), the MLD thickness is greater compared to the summer monsoon months (June-September).
Suggested Reviewers:	Young-Oh Kwon Woods Hole Oceanographic Institution yokwon@whoi.edu The reviewer has a similar research interest and is an expert in this field.
	Elisée Toualy Laboratory of Atmospheric Physics and Fluids Mechanics, Felix Houphouet-Boigny University of Cocody, Abidjan, Cote d'Ivoire elisee.toualy@gmail.com The reviewer has a similar research interest and is an expert in this field.
Opposed Reviewers:	

==========

[Syamsul Rizal,
Universitas Kuala, Banda Aceh, Indonesia]

To:
Editor-in-Chief
OCEANOLOGIA

[20 March 20223]

Dear Professor,
I am pleased to submit an original research article entitled "**Effect of Meteorological Parameters on Mixed Layer Depth in the Bay of Bengal**" by Hidayat et al. for consideration for publication in OCEANOLOGIA.

The study is the detailed investigation of the relationship between five meteorological parameters (AirT, SHum, CPrecR, SLP, and wind stress) and monsoons, as well as mixed layer depth (MLD) in Bay of Bengal (BoB). The study shows that the extreme maximum and minimum of the five selected meteorological parameters follow the peaks and troughs of the northeast monsoon (NEM) and southwest monsoon (SWM), and that MLD thickness follows a seasonal pattern in the northern and southern Bay of Bengal. The finding that MLD thickness is greater during the winter monsoon months compared to the summer monsoon months is also novel.

The research findings have important implications for the relevance of the study to the field. Firstly, the study's detailed investigation of the relationship between meteorological parameters and monsoons provides valuable insights into the complex interactions between the atmosphere and the ocean, and can help improve our understanding of the processes that drive monsoons and their impact on the environment. Secondly, the study's finding that MLD thickness follows a seasonal pattern in the northern and southern Bay of Bengal is significant because the MLD plays an important role in oceanic processes such as nutrient transport and primary productivity, which in turn have implications for marine ecosystems and fisheries. Finally, the finding that MLD thickness is greater during the winter monsoon months compared to the summer monsoon months has important implications for climate modeling and prediction. This information can be used to improve the accuracy of climate models, which can in turn help policymakers make better decisions regarding climate change adaptation and mitigation strategies. Overall, the research findings have important implications for the field of oceanography, atmospheric science, and climate modeling, and can contribute to our understanding of the complex interactions between the atmosphere and the ocean, as well as their impact on the environment and human societies.

I believe that this work aligns well with the scope and focus of OCEANOLOGIA. The study's results are significant and will make a meaningful contribution to the scientific community.

This manuscript has not been published and currently is not under consideration for publication elsewhere.

Thank you for your consideration.

Sincerely,

Effect of Meteorological Parameters on Mixed Layer Depth in the Bay of Bengal

Muh. Nur Hidayat[a], Muhammad Ikhwan[b], Reza Wafdan[c], Marwan Ramli[b], Zainal Abidin Muchlisin[a,d,e], Syamsul Rizal[a,c,e,*]

[a]*Graduate School of Mathematics and Applied Sciences, Universitas Syiah Kuala, Banda Aceh 23111, Indonesia*

[b]*Department of Mathematics, Universitas Syiah Kuala, Banda Aceh 23111, Indonesia*

[c]*Department of Marine Sciences, Faculty of Marine and Fisheries, Universitas Syiah Kuala, Banda Aceh, 23111, Indonesia*

[d]*Department of Aquaculture, Faculty of Marine and Fisheries, Universitas Syiah Kuala, Banda Aceh 23111, Indonesia*

[e]*Research Center for Marine Sciences and Fisheries, Universitas Syiah Kuala, Banda Aceh 23111, Indonesia*

*Corresponding author: srizal@usk.ac.id (S. Rizal)

Abstract

Monsoon winds exert a significant influence on both atmospheric and oceanic conditions. In the ocean, these winds stir the water column, resulting in a thickened mixed layer and a thermocline layer at deeper depths. This vertical layer is characterized by changes in the temperature of the water column. In this study, we investigated in detail the relationship between five meteorological parameters - air temperature (AirT), specific humidity (SHum), convective precipitation rate (CPrecR), sea level pressure (SLP), and wind stress (TauX and TauY) - and monsoons and mixed layer depth (MLD). Results from the analysis of the seasonal model indicate that the extreme maximum and minimum of the five selected meteorological parameters follow the peaks and troughs of the northeast monsoon (NEM) and southwest monsoon (SWM). In the northern and southern Bay of Bengal (BoB), the MLD followed a seasonal pattern, with almost identical thicknesses in both regions. The study also found that during the winter monsoon months (November-February), the MLD thickness is greater compared to the summer monsoon months (June-September).

Keywords: Mixed layer depth, monsoon, meteorological parameters, seasonal model, Bay of Bengal

1. Introduction

The Bay of Bengal (BoB) is a basin-shaped sea located along the Indian subcontinent, Southeast Asia, and the northern Indian Ocean (as shown in Fig. 1). The climate of this region is dominated by monsoons, with the northeast monsoon occurring from November to February, signaling the winter season, and the southwest monsoon

occurring from June to September, marking the summer season (Goswami et al., 2016; Gadgil et al., 1984).

Fig 1.

The interaction between the ocean and atmosphere is a complex and nonlinear process. Meteorological parameters such as wind blowing over the sea surface transfer momentum and mechanical energy to the water, resulting in waves and currents. The oceans, in turn, give off energy as heat, which is emitted through electromagnetic radiation, conduction, and evaporation. Heat flux from the ocean provides a significant energy source for atmospheric movement. The strength of this coupling depends on the interaction between the ocean and atmosphere, which occurs through a small-scale process. The coupling is affected by turbulence at the air/sea interface and the spatial distribution of high and low energy transfer centers influenced by ocean currents. All meteorological parameters that relate to the ocean directly contribute to the mixed layer and have a wide geographic and temporal scale (United Nations [UN], 2016).

Mixed layers can be based on different parameters, such as temperature, and can represent averages over different time intervals, such as days and months (de Boyer Montégut, 2004). Previous research has shown that the MLD has an impact on climate, regulating the response of the mean tropical SST to global warming (Yeh et al., 2009), the shallowing of MLD in the winter season (Yeh et al., 2009; Richards et al., 2021), and the magnitude of sea surface warming (Hwang et al., 2017). Coastal upwelling plays an important role in regional climate through the interaction between the air and the mixed layer (ML) (Bessa et al., 2020; Toualy et al., 2022). Therefore, it is essential to study MLD further to understand its influence and the interactions that can occur in MLD.

In this study, the MLD definition was based on ocean temperature. Sea Surface Temperature (SST) and wind speed can be used as indicators of seasonal changes, while the average MLD has remained unchanged (Muller-Karger et al., 2015). Several other studies have investigated MLD using ocean temperature, including research on MLD using temperature with the threshold method $\Delta t = 0.2^{o}C$ (Jeong et al., 2019). Using the same threshold, the seasonal cycle and spatial patterns can be determined from the MLD (Cai et al., 2021). The threshold criteria used can vary and can be compared with the gradient method. The determination of MLD by temperature with a threshold value

of 1°C is the best method in a specific area after comparing several criteria values and gradient values (Nahavandian et al., 2022). However, the optimal estimation of turbulent mixing penetration is obtained using the threshold criterion of 0.8°C (Kara et al., 2000).

Studies on the influence of meteorological parameters on the MLD have been conducted. Some of the related studies are Toualy et al. (2022), who identified wind parameters in MLD variations, where shallower ML and highly productive seas are observed during cooling periods, while deeper MLD and less productive oceans occur during summer. Kantha et al. (2019) used the mooring Woods Hole Oceanographic Institution (WHOI) data, including wind speed, wind direction, air temperature, relative humidity, precipitation, sea surface temperature, and several other data to drive a one-dimensional mixing model based on the closing turbulence model second moment, to explore the intra-annual variability in the upper layers. Furthermore, it is known that the wind has a direct impact on the MLD, where wind strength simultaneously affects the MLD condition. On the other hand, precipitation shows an indirect impact on MLD. Precipitation takes time to accumulate effects that change the state of the MLD. The time required for precipitation is two months before the MLD changes occur (Ikhwan et al., 2022).

Based on this explanation, the study aims to observe the mixed layer depth (MLD) based on five meteorological parameters, namely air temperature (AirT), specific humidity (SHum), convective precipitation rate (CPrecR), sea level pressure (SLP), and wind stress (TauX and TauY) at the Bay of Bengal (BoB) at latitudes 9°N and 19°N. Fig. 2 shows an illustration of the interactions that occur at the air-sea interface involving meteorological parameters and mixed layer depth. The five meteorological parameters were chosen because HYCOM uses them as external forcing. However, many other meteorological parameters used by HYCOM have not been investigated in this study, and additional parameters are recommended for further study. A seasonal model was used to predict the contribution of each meteorological parameter. As far as the authors know, a detailed study of the meteorological parameters and their impact on the MLD at these two latitudes has never been carried out.

Thus, the purpose of this study was to provide a comprehensive view of the impact of five meteorological parameters, namely AirT, SHum, CPrecR, SLP, and wind stress

(TauX and TauY) on MLD. Specifically, the following research questions were addressed:

1. What is the relationship between monsoon and MLD?

2. What is the relationship between the monsoon and the five selected meteorological parameters?

3. Of the five meteorological parameters, which parameters are directly proportional and which are inversely proportional to the MLD?

4. What is the relationship between MLD and the five parameters seasonally?

Fig. 2

In order to find out whether there are significant differences between the northern and southern BoB, regarding the four questions above, we conducted a study and made vertical transect profiles of temperature along latitudes 9°N and 19°N. These are described in Section 3.2 (The vertical transect profiles of temperature).

To answer the first question, we determined the MLD from the HYCOM data, and the procedure is described in Section 2.3 (Determining the MLD). Meanwhile, to answer the second question, we use NCEP reanalysis data for 20 years from 2002 to 2021, and this is described in Section 2.3 as well. To answer questions 3 and 4, we used the seasonal model as described in Section 3.5 (Seasonal models). To validate the data used, we compared it with OMNI and RAMA measurement data, as described in Section 3.4 (Data validation).

2. Materials and methods

2.1. Materials

The research domain covers the Bay of Bengal (BoB), Andaman waters, and the Indian Ocean with coordinates 5.5°N – 24.6°N and 78.2°E – 96.7°E (see Fig. 1). The research examined the vertical layer variability based on meteorological data at two different latitudes: to the south of the domain at 9°N latitude and to the north at 19°N latitude. This study used elevation and surface current data, as well as temperature data obtained from the HYCOM data analysis model (Naval Research Laboratory, 2014-2022). The HYCOM model is a high-resolution computer model developed from the Miami Isopycnic Coordinate Ocean Model (MICOM), which contains hydrostatic

primitive equations and can be used to model general ocean circulation phenomena (Bleck, 2002). The vertical coordinates in HYCOM are isopycnal in the stratified open ocean, have smooth and dynamic transitions, and are time-dependent in shallow coastal terrain and at constant pressure levels in mixed surface layers or unstratified oceans (Chassignet & Xu, 2017). These temperature data were used to estimate the mixed layer depth at two different latitudes (9°N and 19°N) in the 12-month domain.

Meteorological data used in NCEP/NCAR reanalysis data per 6 hours (https://psl.noaa.gov/data/gridded/data.ncep.reanalysis.html) for 20 years from 2002 to 2021 for five parameters: 2m air temperature (AirT), 2m specific humidity (SHum), convective precipitation rate (CPrecR), and wind stress (TauX and TauY).

2.2. Data validation

This study used temperature data from the HYCOM model and meteorological data from NCEP/NCAR to analyze the parameters affecting the MLD's thickness. HYCOM data have been frequently used in research and have also been widely validated (Metzger et al., 2020; Chassignet et al., 2009; Hall et al., 2022). It was previously known that NCEP/NCAR has biases and errors (Dey et al., 2017; Fu et al., 2016; Cui et al., 2012; Saha et al., 2010); therefore, validation of these data is presented to test the accuracy of the data used by comparing it with the Ocean Moored buoy Network for Northern Indian (OMNI) and Research Moored Array for African-Asian-Australian Monsoon Analysis (RAMA) data. In addition, the Specific Humidity parameter in NCEP/NCAR was converted into Relative Humidity (Bolton, 1980) using the following formula,

$$e_s = 6.112 \times exp\left(\frac{17.67 \times AirT}{AirT + 243.5}\right), e = \frac{SHum \times press}{(0.378 \times SHum + 0.622)}, RelH = \frac{e}{e_s}.$$

With *RelH* is relative humidity, e_s is saturation vapor pressure (in millibars (mb)), *e* is vapor pressure (in mb), *AirT* is Air Temperature (in °C), *press* is surface pressure (equals 1013.25 in mb), and *SHum* is specific humidity (in kg/kg).

2.3. Determination of the mixed layer depth

MLD was determined using HYCOM temperature data from the cross-section depiction in the southern part of the BoB, at 9°N latitude, and the northern part of the BoB, at 19°N latitude. The cross-section temperature uses a finite difference criterion, in particular, the criteria for the threshold temperature value, $\Delta t = 0.1$°C, with reference

to the sea surface (Sprintall & Roemmich, 1999). The method used to estimate the thickness of the MLD was based on temperature changes at each depth. The cross-section temperature image is plotted first without a contour using a threshold criterion of 0.1°C to produce images with color gradation representing temperature changes. Contour images were then added to clearly see the temperature values based on 1°C intervals. The indicator for the MLD thickness value was based on the color and temperature changes that occurred for the first time at sea level.

2.4. Seasonal model

The data were interpolated and analyzed using seasonal signals according to the following equation (Hidayat et al., 2023, Haridhi et al., 2016):

$$y = \alpha + \beta\, sin(2\pi t) + \gamma\, cos(2\pi t), \qquad (1)$$

where α is the constant vertical displacement, β is the amplitude of the sine wave, γ is the cosine wave, and t is time. This formula is used to explain seasonal patterns and can also predict MLD parameters and events based on their regularity (Ikhwan et al., 2022). The choice of season using this formula affects the suitability of the monsoon that occurs. In the Andaman Sea and the Malacca Strait, the monsoons that occur are the northeast monsoon (NEM) and the southwest monsoon (SWM) therefore, this monsoon assumption can also occur in the BoB (Rizal et al., 2012).

3. Results and discussion

3.1. Wind circulations

The wind figure is presented in Fig. 3, where wind stress is represented by arrows (in Pa), and the color gradation indicates wind speed (in m/s). In February (Fig. 3a), the wind blows from the northeast to the southwest, while in August (Fig. 3b), the wind blows from the southwest to the northeast.

Fig. 3

3.2. The vertical transect profiles of temperature

Instead of using the sample location, this study uses the cross-section of temperature to provide ideas and descriptions regarding the location of the highest temperature gradient, resulting in more comprehensive results. Fig. 4 presents the cross-sectional temperature to show the depth of the well-mixed layer in the south of the BoB (latitude

9°N) and north of the BoB (latitude 19°N) for 12 months in 2021. Table 1 shows the MLD depth estimations derived from Fig. 4.

The criterion used to describe the MLD in the maps in Fig. 4 is the temperature threshold value of 0.1°C. First, cross-section images are plotted without contours using this criterion to produce images with different colors of blue, green, and yellow. Then, contour images are added to view the temperature values. The indicator for the MLD thickness value is based on a temperature of 25°C with orange color in the picture. Fig. 4 shows a cross-section of ocean temperature (in °C) at latitude 9°N and latitude 19°N for 12 months in 2021. The cross-section is described using the relationship between longitude (x-axis, in degrees) and depth (y-axis, in meters). Temperature values vary based on longitude and depth, depicted by contours and colorbars. The colorbar is fixed from a value range of 0 – 30°C, and the depth is limited from 0-150 meters to make the figure readable.

Similarly, the northern part of the BoB in Fig. 4b also shows four contrasting colors (light blue, green, orange, and yellow). At a depth of 0-50 m, temperature values range from 27°C to 30°C, marked with yellow color and contours in the figure. At depths of 50-100m, temperature values range from 24°C to 27°C, marked in green and orange, except for the last few months (September to December), which can reach around 22°C to 27°C. Finally, at a depth of 100 – 150 m, the temperature values range from 16°C to 24°C from January to August and 17°C to 22°C from September to December, marked in light blue.

Table 1

Fig. 4

Based on the previously defined MLD thickness indicators, the estimated MLD thickness values can be found in Table 1. The MLD thickness values are provided within an interval to accommodate varying thickness values based on different longitudes. Table 1 shows that the MLD value at latitude 9°N can have a thickness value ranging from 60 m to 100 m. It appears that the variation of MLD thickness along longitude is quite large in March and December, reaching 35 m. Additionally, this month, the shallowest MLD occurred at 60 m. The deepest MLD is shown in February and November, which is 100 m.

On the other hand, latitude 19°N in Table 1 shows that the MLD thickness varies from 50 m to 105 m. MLD thickness variation along longitude can reach 55 m, which occurs in March. It also appears that the shallowest MLD values occur in March, May, and June, which are 50 m, while the deepest MLD is shown in March and April, which is 105 m. If the MLD variation values at both latitudes are averaged, latitude 19°N shows the most considerable MLD thickness variation, 28.3 m, compared to the MLD thickness variation at latitude 9°N, which is only 23.3 m.

Table 2

Table 2 presents the values of the average lower limit (Min$\overline{\mathbf{X}}$) and upper limit (Max$\overline{\mathbf{X}}$), at latitude 9^{o}N and 19^{o}N in winter monsoon months (November-February) and summer monsoon months (June-September). The formula used to find the Min$\overline{\mathbf{X}}$ and Max$\overline{\mathbf{X}}$ values are as follows

$$\text{Min}\overline{\mathbf{X}} = \frac{\sum \text{Min}\boldsymbol{X_i}}{4}, \text{Max}\overline{\mathbf{X}} = \frac{\sum \text{Max}\boldsymbol{X_i}}{4},$$

where *i* is the number of winter or summer monsoon months. Table 2 shows that the thickness of the MLD layer is thicker in the winter monsoon than in the summer monsoon, both for the minimum and maximum depths. These apply for both latitudes, latitude 9^{o}N and latitude 19^{o}N.

3.3. The extreme values of 5 selected meteorological parameters

Five parameters of atmospheric forces were analyzed, and the visualization results of these parameters for the southern BoB (latitude 9^{o}N) and northern BoB (latitude 19^{o}N) over 20 years from 2002 to 2021 are presented in Fig. 5. The annual extreme values of these parameters for both research domains are shown in Appendix A and Appendix B, which are useful for determining the peaks and troughs of each meteorological parameter. The purpose of Fig. 5 is to observe the repeatability (periodicity) of the five parameters studied, while Appendix A and Appendix B are derived from Fig. 5 to present the data quantitatively. These extreme values are essential to determine in which month they occur and are used as a reference to analyze the five meteorological parameters affecting the occurrence of these extreme values.

Overall, the trends of three parameters, namely AirT, SHum, and wind stress (TauX and TauY), have minimum values in winter or December to February and maximum values in late spring and summer from May to August. On the other hand, the trend of

the remaining two parameters, CPrecR and SLP, has a minimum value in late spring and summer, from May to July, and a maximum value in winter, from December to February.

It is noteworthy that the minimum average value of the five parameters, namely AirT, SHum, CPrecR, SLP, and wind stress (TauX and TauY), at latitude 9^{o}N is 25.47, 0.015, -0.0003, 100.2, -0.15, and -0.11, respectively. At the same time, the maximum average value of the five parameters in a row is 30.53, 0.022, 0, 101.61, 0.225, and 0.18, respectively. In comparison to the extreme values at latitude 19^{o}N, the difference between the minimum and maximum values at latitude 19^{o}N is greater than at latitude 9^{o}N. As a result, the extreme value between the two domains studied is higher at latitude 19^{o}N. Furthermore, at latitude 19^{o}N, the minimum average value for the five parameters is 20.99, 0.009, -0.0004, 99.57, -0.11, and -0.11, respectively, while the average maximum value for the five parameters is 31.2, 0.023, 0.102, 0.196, and 0.231, respectively.

3.4. Data validation

Fig. 6 shows a comparison of temperature data from HYCOM (solid black line) with OMNI data (dashed red line) at three coordinate stations, namely coordinates (84.17^{o}E,13.53^{o}N), (87.99^{o}E,16.36^{o}N), and (87^{o}E,13.99^{o}N). Ocean temperatures are compared from February to December 2021 with depth values of 1m, 10m, 50m, and 100m. The HYCOM temperature value at station 2 (Fig. 6b) is slightly different from the OMNI data, especially for July (0m, 10m, and 50m depth) and 50m depth. The comparison results generally show that the HYCOM temperature data has a trend and line pattern similar to the OMNI temperature data.

Fig. 7 shows NCEP/NCAR meteorological data validation against OMNI and RAMA data. Fig. 7 compares three meteorological parameters, namely Air Temperature, Relative Humidity, and Wind Speed at three different stations (St. 1-3) from February to December 2021 and the meteorological parameter Sea Level Pressure at the fourth station from September 2020 until July 2021. The Specific Humidity parameter in NCEP/NCAR is converted into Relative Humidity (Bolton, 1980). The comparison results show that the NCEP/NCAR meteorological data has a trend and line pattern similar to the OMNI and RAMA data. However, the OMNI data for Relative Humidity at station 1 does not match the Relative Humidity data at NCEP/NCAR.

The RMSE value in Fig. 8 is calculated to see the error and bias resulting from comparing temperature and meteorological data. Fig. 8a shows the RMSE for temperature data at three stations in Fig. 6. The 100m depth at station 2 is ignored in this figure because OMNI does not have data for December 2021. The calculation results show that the temperature value has fairly high accuracy, especially at a depth of 1m and 10m at three station locations.

Fig. 8b shows the RMSE of meteorological data for each station in Fig. 7. The calculation results show that the Air Temperature, Sea Level Pressure, and Wind Speed parameters have a fairly high level of accuracy compared to the Relative Humidity parameter. Relative Humidity at the first station has a relatively high error.

Fig. 5

Fig. 6

Fig. 7

Fig. 8

3.5. Seasonal model

The data for 20 years (2002-2021) in Fig. 5 were observed to determine seasonal models in both domains (latitude 9^{o}N and latitude 19^{o}N) and aimed to identify extreme seasonal points each year. The results of the 20-year seasonal model are presented for the last two years (2020-2021) in Fig. 9. For additional information, Table 4 summarizes the values of the extreme points from 2002-2021 based on the seasonal model obtained.

Table 3

Table 3 shows the results of the seasonal model analysis from equation (1) for atmospheric forces. The constant (α) is a fixed value that is not affected by the season, while the coefficients (β) and (γ) are variables that are influenced by the season. Furthermore, the constant values in Table 3 and equation (1) describe the prediction model for 20 years, and the results are shown in Fig. 9.

The average value (α) in Table 3 shows that the AirT value is higher at 9^{o}N latitude than at 19^{o}N latitude. The same trend is observed for the SHum and TauX parameters. In contrast, the CPrecR and TauY parameters are higher at 19^{o}N latitude than at 9^{o}N latitude. Moreover, for the SLP parameter, the values are the same in both locations.

Fig. 9

From Table 4 and Fig. 9, it can be observed that the five forces studied, namely AirT, SHum, CPrecR, SLP, and wind stress (TauX and TauY), influence the domains taken as research samples. Of the five parameters, the average extreme values in both domains occur in February and August each year in the prediction model obtained. The three parameters AirT, SHum, and wind stress (TauX and TauY) show the same trend: the minimum in February and the maximum in August. In contrast to the trend of parameters CPrecR and SLP, the minimum occurs in August, and the maximum occurs in February. All five meteorological parameters examined, including extreme minimum and maximum, occur in the winter and summer monsoons.

Table 4

4. Summary and conclusion

A description of the temperature-based MLD seasonal cycle has been constructed using temperature data from HYCOM. The MLD definition used in this study follows the threshold method, $\Delta t=0.1°C$, with reference to the sea surface. Then, from the meteorological parameters of NCEP/NCAR, a seasonal model is formed to identify the parameters that affect the thickness of the MLD. This seasonal model is very useful for estimating peaks and troughs from meteorological parameters (Toharudin et al., 2021; Yates et al., 2020; Ikhwan et al., 2022; Haridhi et al., 2016). In addition, temperature data and meteorological data were validated by comparing them with OMNI/RAMA in situ data.

The results of this study indicate that the monsoon plays a significant role in the thickness of MLD. This is evident from the average lower limit (Min$\overline{\mathbf{X}}$) and upper limit (Max$\overline{\mathbf{X}}$) MLD values shown in Table 2, where the MLD is thicker during the winter monsoon months (November-February) than in the summer monsoon months (June-September). These findings apply to both latitudes: latitude 9°N and latitude 19°N.

The results of the seasonal model show that three parameters, namely Air Temperature, Specific Humidity, and Wind Stress, occur with an extreme minimum in December and January and an extreme maximum in June and July. With respect to MLD, the extreme minimum of these three parameters contributes positively to the thickness of MLD, while their extreme maximum makes the MLD thinner in the

summer months. These findings apply to both latitudes because these three parameters are inversely proportional to the MLD.

For the other two parameters, the extreme minimum of Convective Precipitation Rate and Sea Level Pressure occurs in July and August, respectively, which contributes to the thinness of the MLD layer. Meanwhile, in January and February, respectively, these parameters occur at extreme maximums, contributing to a thicker MLD. These findings also apply to both latitudes because these two parameters are directly proportional to the MLD.

The seasonal model for five meteorological parameters suggests that extreme maximum and minimum values are only observed during the winter monsoon (December-February) and summer monsoon (June-August) seasons. Consequently, the conclusion can be drawn that all meteorological parameters conform to the monsoon season.

It is recommended that further research should be conducted to investigate other meteorological parameters, such as heat flux, long and short-wave radiation, freshwater flux, cloud cover, and other parameters.

Data Availability Statement

The HYCOM temperature data analyzed in this paper are available for download https://www.hycom.org/dataserver/gofs-3pt1/analysis. The NCEP/NCAR data are obtained from https://psl.noaa.gov/data/gridded/data.ncep.reanalysis.html. The OMNI/RAMA data are downloaded from https://incois.gov.in/portal/datainfo/buoys.jsp.

Declaration of Competing Interest

The authors declare that they have no known competing financial interests or personal relationships that could have appeared to influence the work reported in this paper.

Data availability

Data will be made available on request.

Acknowledgments

This research was funded by the scheme of “Penelitian Profesor (PP)” for the 2021 fiscal year with the contract number [7/UN11.2.1/PT.01.03/PNBP/2021] and the “Penelitian Pendidikan Magister menuju Doktor untuk Sarjana Unggul (PMDSU)”

scheme for the 2022 fiscal year with contract number [97/UN11.2.1/PT.01.03/DPRM/2022]. The authors would like to thank the Ocean Modeling Laboratory, Department of Marine Sciences, Universitas Syiah Kuala, Indonesia, for providing research facilities.

Appendix A

Appendix B

References

Bessa, I., Makaoui, A., Agouzouk, A., Idrissi, M., Hilmi, K., Afifi, M., 2020. Variability of the ocean mixed layer depth and the upwelling activity in the Cape Bojador, Morocco. Modeling Earth Systems and Environment, 6(3), 1345–1355. https://doi.org/10.1007/s40808-020-00774-1.

Bleck, R., 2002. An oceanic general circulation model framed in hybrid isopycnic-Cartesian coordinates. Ocean Modelling, 4(1), 55–88. https://doi.org/10.1016/S1463-5003(01)00012-9.

Bolton, D., 1980. The Computation of Equivalent Potential Temperature. Monthly Weather Review, 108(7), 1046–1053. https://doi.org/10.1175/1520-0493(1980)108<1046:TCOEPT>2.0.CO;2.

Cai, C., Kwon, Y.-O., Chen, Z., Fratantoni, P., 2021. Mixed layer depth climatology over the northeast U.S. continental shelf (1993–2018). Continental Shelf Research, 231, 104611. https://doi.org/10.1016/j.csr.2021.104611.

Chassignet, E.P., Hurlburt, H.E., Metzger, E.J., Smedstad, O. M., Cummings, J. A., Halliwell, G. R., Bleck, R., Baraille, R., Wallcraft, A.J, Lozano, C., Tolman, H.L, Srinivasan, A., Hankin, S., Cornillon, P., Weisberg, R., Barth, A., He, R., Werner, F., Wilkin, J., 2009. US GODAE: global ocean prediction with the HYbrid Coordinate Ocean Model (HYCOM). Oceanography, 22(2), 64-75.

Chassignet, E.P., Xu, X., 2017. Impact of Horizontal Resolution (1/12° to 1/50°) on Gulf Stream Separation, Penetration, and Variability. Journal of Physical Oceanography, 47(8), 1999–2021. https://doi.org/10.1175/JPO-D-17-0031.1.

Cui, B., Toth, Z., Zhu, Y., Hou, D., 2012. Bias Correction for Global Ensemble Forecast. Weather and Forecasting, 27(2), 396–410. https://doi.org/10.1175/WAF-D-11-00011.1.

de Boyer Montégut, C., 2004. Mixed layer depth over the global ocean: An examination of profile data and a profile-based climatology. Journal of Geophysical Research, 109(C12), C12003. https://doi.org/10.1029/2004JC002378.

Dey, D., Sil, S., Jana, S., Pramanik, S., Pandey, P.C., 2017. An assessment of TropFlux and NCEP air-sea fluxes on ROMS simulations over the Bay of Bengal region. Dynamics of Atmospheres and Oceans, 80, 47–61. https://doi.org/10.1016/j.dynatmoce.2017.09.002.

Fu, G., Charles, S.P., Timbal, B., Jovanovic, B., Ouyang, F., 2016. Comparison of NCEP-NCAR and ERA-Interim over Australia. International Journal of Climatology, 36(5), 2345–2367. https://doi.org/10.1002/joc.4499.

Gadgil, S., Joseph, P.V., Joshi, N.V., 1984. Ocean–atmosphere coupling over monsoon regions. Nature, 312(5990), 141–143. https://doi.org/10.1038/312141a0.

Goswami, B.N., Rao, S., Sengupta, D., Chowdary, S., 2016. Monsoons to Mixing in the Bay of Bengal: Multiscale Air-Sea Interactions and Monsoon Predictability. Oceanography, 29(2), 18–27. https://doi.org/10.5670/oceanog.2016.35.

Hall, K., Daley, A., Whitehall, S., Sandiford, S., Gentemann, C.L., 2022. Validating Salinity from SMAP and HYCOM Data with Saildrone Data during EUREC4A-OA/ATOMIC. Remote Sensing, 14(14), 3375. https://doi.org/10.3390/rs14143375.

Haridhi HA, Nanda M, Wilson CR, Rizal S. (2016). Preliminary study of the sea surface temperature (SST) at fishing ground locations based on the net deployment of traditional purse-seine boats in the northern waters of Aceh - A community-based data collection approach. Reg Stud Marine Sci 8:114–121. https://doi.org/10.1016/j.rsma.2016.10.002.

Hidayat, M. N., Wafdan, R., Ramli, M., Muchlisin, Z. A., Rizal, S., 2023. Relationship between chlorophyll-a, sea surface temperature, and sea surface salinity. Global Journal of Environmental Science and Management. https://doi.org/10.22034/gjesm.2023.03.09.

Hwang, Y.-T., Xie, S.-P., Deser, C., Kang, S. M., 2017. Connecting tropical climate change with Southern Ocean heat uptake. Geophysical Research Letters, 44(18), 9449–9457. https://doi.org/10.1002/2017GL074972.

Ikhwan, M., Haditiar, Y., Wafdan, R., Ramli, M., Muchlisin, Z. A., Rizal, S., 2022. Seasonal variability of mixed layer depth in the Andaman Sea. International Journal of Environmental Science and Technology. https://doi.org/10.1007/s13762-022-03976-5.

Jeong, Y., Hwang, J., Park, J., Jang, C. J., Jo, Y.-H., 2019. Reconstructed 3-D Ocean Temperature Derived from Remotely Sensed Sea Surface Measurements for Mixed Layer Depth Analysis. Remote Sensing, 11(24), 3018. https://doi.org/10.3390/rs11243018.

Kantha, L., Weller, R.A., Farrar, J.T., Rahaman, H., Jampana, V., 2019. A note on modeling mixing in the upper layers of the Bay of Bengal: Importance of water type, water column structure and precipitation. Deep Sea Research Part II: Topical Studies in Oceanography, 168(April), 104643. https://doi.org/10.1016/j.dsr2.2019.104643.

Kara, A.B., Rochford, P.A., & Hurlburt, H.E., 2000. An optimal definition for ocean mixed layer depth. Journal of Geophysical Research: Oceans, 105(C7), 16803–16821. https://doi.org/10.1029/2000JC900072.

Metzger, E.J., Hogan, P.J., Shriver, J.F., Thoppil, P.G., Douglass, E., Yu, Z., Allard, R.A., Rowley, C.D., Smedstad, O.M., Franklin, D.S., Phelps, M.W., Zamudio, L., Wallcraft, A.J., Richman, J.R., 2020. Validation Test Report for the Global Ocean Forecast System 3.5-1/25o HYCOM/CICE with Tides. https://apps.dtic.mil/sti/citations/AD1113389.

Muller-Karger, F.E., Smith, J.P., Werner, S., Chen, R., Roffer, M., Liu, Y., Muhling, B., Lindo-Atichati, D., Lamkin, J., Cerdeira-Estrada, S., Enfield, D.B., 2015. Natural

variability of surface oceanographic conditions in the offshore Gulf of Mexico. Progress in Oceanography, 134, 54–76. https://doi.org/10.1016/j.pocean.2014.12.007.

Nahavandian, S., Jannar Fereidouni, F., Mahmoudi, N., 2022. On the seasonal variability of the vertical physical structure of the water column in the continental shelf, South-Eastern Caspian Sea. Journal of Sea Research, 187, 102246. https://doi.org/10.1016/j.seares.2022.102246.

Naval Research Laboratory., 2014–2022. Global Ocean Forecast System (GOFS) 3.1 [Dataset]. https://www.hycom.org/dataserver/gofs-3pt1/analysis.

Richards, K. J., Whitt, D. B., Brett, G., Bryan, F. O., Feloy, K., Long, M. C., 2021. The Impact of Climate Change on Ocean Submesoscale Activity. Journal of Geophysical Research: Oceans, 126(5), e2020JC016750. https://doi.org/10.1029/2020JC016750.

Rizal, S., Damm, P., Wahid, M. A., Sündermann, J., Ilhamsyah, Y., Iskandar, T., 2012. General circulation in the Malacca strait and Andaman Sea: a numerical model study. American Journal of Environmental Sciences, 8(5), 479-488.

Saha, S., Moorthi, S., Pan, H.-L., Wu, X., Wang, J., Nadiga, S., Tripp, P., Kistler, R., Woollen, J., Behringer, D., Liu, H., Stokes, D., Grumbine, R., Gayno, G., Wang, J., Hou, Y.-T., Chuang, H., Juang, H.-M.H., Sela, J., Iredell, M., Treadon, R., Kleist, D., Delst, P.VDennis Keyser, D., Derber, J., Ek, M., Meng J., Wei, H., Yang R., Lord S., den Dool, H.V, Kumar A., Wang W., Long C., Chelliah, M., Xue Y., Huang, B., Schemm, J.-K, Ebisuzaki, W., Lin, R., Xie, P., Chen, M., Zhou, S., Higgins, W., Zou, C.-Z., Liu, Q., Chen, Y., Han, Y., Cucurull, L., Reynolds, R.W., Rutledge, G., Goldberg, M., 2010. The NCEP Climate Forecast System Reanalysis. Bulletin of the American Meteorological Society, 91(8), 1015–1058. https://doi.org/10.1175/2010BAMS3001.1.

Sprintall, J., Roemmich, D., 1999. Characterizing the structure of the surface layer in the Pacific Ocean. Journal of Geophysical Research: Oceans, 104(C10), 23297–23311. https://doi.org/10.1029/1999JC900179

Toharudin, T., Pontoh, R.S., Caraka, R.E., Zahroh, S., Lee, Y., Chen, R.C., 2021. Employing long short-term memory and Facebook prophet model in air temperature forecasting. Communications in Statistics - Simulation and Computation, 1–24. https://doi.org/10.1080/03610918.2020.1854302

Toualy, E., Kouacou, B., Aman, A., 2022. Influence of Wind and Surface Buoyancy Flux on the Variability of the Oceanic Mixed Layer Depth in the Northern Gulf of Guinea Coastal Upwelling. Thalassas: An International Journal of Marine Sciences, 38(1), 599–608. https://doi.org/10.1007/s41208-021-00358-5

United Nations [UN], 2016. The First Global Integrated Marine Assessment. World Ocean Assessment I. Cambridge: Cambridge University Press.

Yates, C., MacDermott, H., Evans, J., Murphy, B.P., Russell-Smith, J., 2020. Seasonal fine fuel and coarse woody debris dynamics in north Australian savannas. International Journal of Wildland Fire, 29(12), 1109. https://doi.org/10.1071/WF20073

Yeh, S.-W., Yim, B.Y., Noh, Y., Dewitte, B., 2009. Changes in mixed layer depth under climate change projections in two CGCMs. Climate Dynamics, 33(2–3), 199–213.

Highlights

- The MLD is thicker during the winter monsoon months (November-February) than in the summer monsoon months (June-September) both for latitude 9^{o}N and latitude 19^{o}N.
- The parameters of Air Temperature, Specific Humidity, and Wind Stress occur at extreme minimum in December and January and extreme maximum in June and July.
- The parameters for Convective Precipitation Rate and Sea Level Pressure occur at extreme minimum in July and August and extreme maximum in January and February.
- The pattern of Air Temperature, Specific Humidity, and Wind Stress is inversely proportional to the MLD pattern, while the Convective Precipitation Rate and Sea Level Pressure is directly proportional to the MLD pattern.

Table 1. MLD thickness estimation (in meters) for 12 months in 2021

Domain	Months											
	1	**2**	**3**	**4**	**5**	**6**	**7**	**8**	**9**	**10**	**11**	**12**
Latitude 9ºN	75-90 m	70-100 m	60-95 m	70-95 m	70-85 m	70-85 m	65-90 m	65-85 m	65-80 m	65-80 m	70-100 m	60-95 m
Latitude 19ºN	80-100 m	60-100 m	50-105 m	65-105 m	50-85 m	50-95 m	65-85 m	60-85 m	70-85 m	75-85 m	75-100 m	75-85 m

MLD values were estimated from Fig. 4 based on temperature 25ºC with orange color as an indication of MLD thickness.

Table 2. Average MLD thickness (in meters) based on Monsoon

	Winter (Nov-Feb)		**Summer (Jun-Sep)**	
	Min$\overline{X}$	Max$\overline{X}$	Min$\overline{X}$	Max$\overline{X}$
Latitude 9ºN	68.75	96.25	66.25	85
Latitude 19ºN	72.5	96.25	61.25	87.5

The average MLD thickness is calculated from Table 1 by averaging the minimum and maximum thickness of the MLD layer by season.

Table 3. Constant and coefficient of predictor y

Parameters	Latitude 9ºN			Latitude 19ºN		
	α	β	γ	α	β	γ
AirT	28.125762	0.219930	-0.770494	27.131780	-0.479135	-2.352771
SHum	1.941e-02	-2.133e-04	-8.554e-04	1.811e-02	-1.194e-03	-4.624e-03
CPrecR	-6.752e-05	2.286e-05	7.285e-06	-5.242e-05	3.976e-05	6.407e-05
SLP	1.009e+02	4.803e-02	1.890e-01	1.009e+02	1.277e-01	6.030e-01
TauX	0.0197177	-0.0259651	-0.0737232	0.0181436	0.0034581	-0.0291363
TauY	0.0189324	-0.0210637	-0.0609275	0.0213336	0.0037017	-0.0511181

Table 4. Extreme value for the seasonal model

Domain	Year(s)	Extreme	AirT	Shum	CPrecR	SLP	TauX	TauY
Latitude 9ºN	**2002 – 2021**	Min	Dec	Jan	Aug	Jul	Jan	Jan
		Max	Jun	Jul	Feb	Jan	Jul	Jul
Latitude 19ºN	**2002 – 2021**	Min	Jan	Jan	Jul	Jul	Jan	Jan
		Max	Jul	Jul	Jan	Jan	Jul	Jul

Appendix A

Years	2m Air Temperature (ºC)				2m Specific Humidity (kg/kg)				Convective Precipitation Rate (kg/m^{2}s)				Sea Level Pressure (kPa)				Wind Stress U (Pa)				Wind Stress V (Pa)			
	Min		Max		Min		Max		Min		Max		Min		Max		Min		Max		Min		Max	
	Valu	Time	Valu	Time	Valu	Time	Valu	Time	Valu	Time	Valu	Time	Valu	Time	Valu	Time	Valu	Time	Valu	Time	Valu	Time	Valu	Time
2002	25.69	Feb	31.00	May	0.0157	Jan	0.0223	May	-0.0003	Nov	0	Jan	100.27	Jun	101.77	Feb	-0.2	Jan	0.199	Sep	-0.11	Jan	0.168	May
2003	25.90	Jan	30.45	May	0.0153	Jan	0.0217	May	-0.0004	May	0	Jan	100.21	May	101.58	Jan	-0.18	Dec	0.214	Aug	-0.1	Dec	0.194	May
2004	25.33	Feb	30.32	Apr	0.0150	Feb	0.0215	May	-0.0003	May	0	Jan	100.34	Aug	101.58	Feb	-0.2	Dec	0.22	May	-0.09	Dec	0.155	May
2005	25.80	Dec	30.69	May	0.0158	Mar	0.0217	May	-0.0003	Sep	0	Jan	100.19	Sep	101.72	Mar	-0.16	Jan	0.251	Jul	-0.1	Jan	0.204	Jul
2006	25.30	Jan	30.69	Apr	0.0140	Jan	0.0222	Apr	-0.0003	May	0	Jan	100.22	Jun	101.58	Jan	-0.18	Dec	0.226	Jul	-0.11	Dec	0.171	Jul
2007	25.49	Jan	30.47	May	0.0141	Mar	0.0220	May	-0.0003	Jun	0	Jan	100.06	Jun	101.62	Feb	-0.18	Jan	0.177	Jul	-0.14	Jan	0.16	Jul
2008	25.84	Jan	30.09	May	0.0159	Jan	0.0217	May	-0.0003	Apr	0	Jan	100.29	Aug	101.52	Feb	-0.11	Nov	0.215	Jul	-0.1	Dec	0.204	Jul
2009	24.93	Jan	30.35	May	0.0157	Jan	0.0218	May	-0.0003	May	0	Jan	100.14	May	101.68	Jan	-0.13	Jan	0.242	Jul	-0.11	Feb	0.18	May
2010	25.58	Dec	30.90	May	0.0152	Feb	0.0226	May	-0.0004	May	0	Jan	100.22	Aug	101.69	Jan	-0.14	Dec	0.186	Jul	-0.13	Jan	0.15	May
2011	25.30	Jan	29.82	Jun	0.0164	Feb	0.0212	May	-0.0003	Dec	0	Feb	100.28	Jul	101.39	Feb	-0.22	Nov	0.222	Jun	-0.13	Jan	0.159	Jul
2012	25.34	Jan	30.22	Apr	0.0158	Mar	0.0216	May	-0.0003	Nov	0	Feb	100.23	Jul	101.52	Jan	-0.13	Dec	0.229	Jun	-0.12	Jan	0.173	May
2013	25.40	Dec	30.65	May	0.0155	Mar	0.0225	May	-0.0004	Nov	0	Jan	100.16	Jun	101.52	Jan	-0.15	Dec	0.215	Jun	-0.11	Dec	0.169	Jul
2014	24.89	Feb	30.48	May	0.0150	Mar	0.0220	Jun	-0.0003	Jul	0	Feb	100.11	Jun	101.62	Jan	-0.16	Dec	0.235	Jul	-0.13	Jan	0.171	Jul

Appendix B

2m Air Temperature (°C)		Years	2m Specific Humidity (kg/kg)			Convective Precipitation Rate (kg/m^{2}s)			Sea Level Pressure (kPa)			Wind Stress U (Pa)			Wind Stress V (Pa)		
Min	Max		Min	Max		Min	Max		Min	Max		Min	Max		Min	Max	
Valu	Time	Average	Valu	Time	Average	Valu	Time	Average	Valu	Time	Average	Valu	Time	Average	Valu	Time	Average
21.70	30.93	25.47	0.0100	0.0239	0.0169	-0.0005	0	-0.0003	99.62	102.08	101.61	-0.19	0.185	-0.15	-0.11	0.171	0.18
Jan	Jun	Jan	Jan	Jun	Jan	Jul	Jan	May	Jul	Jan	Jan	Dec	Aug	Dec	Dec	Jun	Jul
21.41	32.04	25.70	0.0087	0.0228	0.0152	-0.0006	0	-0.0003	99.44	102.00	101.49	-0.11	0.141	-0.12	-0.1	0.19	0.192
Feb	May	Dec	Feb	May	Feb	Jun	Jan	May	May	Jan	Dec	Sep	Jun	Feb	Oct	Aug	Jun
21.33	31.32	25.60	0.0094	0.0233	0.0155	-0.0004	0	-0.0003	99.62	102.08	101.63	-0.15	0.184	-0.14	-0.1	0.214	0.223
Dec	May	Jan	Jan	Jun	Jan	Oct	Jan	May	Jul	Dec	Jan	May	Jun	Feb	Dec	Jun	May
20.88	31.18	25.93	0.0090	0.0230	0.0170	-0.0004	0	-0.0003	99.57	102.08	101.66	-0.06	0.18	-0.12	-0.1	0.167	0.173
Feb	May	Jan	Feb	Jul	Apr	Aug	Jan	Apr	May	Feb	Jan	Nov	Aug	Nov	Feb	Aug	Sep
21.41	32.04	25.67	0.0087	0.0228	0.0150	-0.0006	0	-0.0003	99.44	102.00	101.66	-0.11	0.141	-0.12	-0.1	0.19	0.192
Feb	May	Feb	Feb	May	May	Oct	Jan	May	May	Jan	Feb	Sep	Jun	Mar	Oct	Aug	Jun
24.15	30.64	25.72	0.0100	0.0239	0.0142	-0.0005	0	-0.0003	99.62	102.08	101.66	-0.19	0.185	-0.15	-0.11	0.171	0.18
Feb	May	Jan	Jan	Jun	Jan	Jul	Jan	May	Jul	Dec	Jan	Dec	Aug	Dec	Dec	Jun	Jul
25.79	31.10	30.60	0.0162	0.0225	0.0142	-0.0004	0	-0.0004	99.62	102.08	101.65	-0.19	0.232	-0.15	-0.11	0.206	0.206
Dec	May	May	Jan	May	Feb	Dec	Jan	May	May	Jan	Jan	Jan	Jul	Jan	Jan	May	May
25.72	30.60	30.60	0.0142	0.0219	0.0142	-0.0004	0	-0.0004	99.62	102.08	101.74	-0.13	0.262	-0.11	-0.11	0.19	0.19
Jan	May	May	Jan	May	Feb	Nov	Jan	May	Jul	Jan	Jan	Feb	Jul	Jan	Dec	Jul	Jul

2021	2020	2019	2018	2017	2016	2015	2014	2013	2012	2011	2010	2009	2008	2007	2006
21.54	20.89	20.76	20.08	21.50	19.59	20.19	21.31	20.07	20.85	20.62	21.40	21.84	21.44	20.88	21.56
Feb	Jan	Jan	Jan	Jan	Jan	Jan	Feb	Jan	Jan	Dec	Dec	Jan	Feb	Jan	Jan
31.80	31.21	31.30	30.75	30.85	30.61	31.31	31.76	30.84	31.84	30.90	31.61	31.29	31.20	30.62	30.55
May	May	Jun	Jun	May	Apr	May	Jun	May	Jun	Jun	May	May	May	Jun	May
0.0094	0.0096	0.0095	0.0085	0.0098	0.0094	0.0089	0.0084	0.0078	0.0093	0.0093	0.0090	0.0102	0.0083	0.0085	0.0089
Dec	Jan	Dec	Jan	Jan	Jan	Feb	Feb	Jan	Jan	Jan	Dec	Jan	Feb	Jan	Jan
0.0233	0.0238	0.0237	0.0230	0.0234	0.0229	0.0231	0.0236	0.0229	0.0237	0.0229	0.0236	0.0233	0.0235	0.0232	0.0230
Jun	Aug	Jun	Jun	Jun	Jul	May	Jun	Jun	Jun	Jun	May	Sep	May	May	Jul
-	-0.0005	-0.0006	-0.0005	-0.0004	-0.0004	-0.0005	-0.0006	-0.0005	-0.0003	-0.0004	-0.0004	-0.0005	-0.0004	-0.0006	-0.0005
May	May	Aug	Sep	Oct	Jul	Jun	Jul	Jul	Aug	Sep	Jul	Jul	Oct	Jun	Sep
0	0	0	0	0	0	0	0	0	0	0	0	0	0	0	0
Jan	Jan	Jan	Jan	Jan	Jan	Jan	Jan	Jan	Jan	Jan	Jan	Jan	Jan	Jan	Jan
99.40	99.29	99.46	99.57	99.82	99.61	99.73	99.69	99.67	99.75	99.53	99.65	99.51	99.51	99.42	99.46
May	Aug	Aug	Jul	Jul	Aug	Jun	Jul	Jul	Jun	Jun	Jul	May	Aug	Jun	Jul
102.03	102.11	102.10	101.98	102.11	102.06	102.08	102.13	101.87	101.85	101.83	102.15	102.20	101.82	102.00	101.97
Dec	Jan	Feb	Feb	Feb	Jan	Feb	Jan	Jan	Feb	Jan	Jan	Jan	Feb	Jan	Feb
-0.09	-0.15	-0.1	-0.13	-0.15	-0.07	-0.14	-0.15	-0.15	-0.06	-0.12	-0.13	-0.07	-0.08	-0.13	-0.07
Dec	May	Nov	Oct	Oct	Oct	Jan	Oct	Oct	Nov	Dec	Nov	Nov	Nov	Jun	May
0.229	0.233	0.261	0.189	0.18	0.202	0.223	0.241	0.223	0.203	0.174	0.151	0.166	0.173	0.221	0.152
Aug	Jul	Aug	Jul	Jun	Jun	Aug	Jul	Aug	Jul	Jun	Jun	Jul	Jun	Jul	Jul
-0.1	-0.1	-0.09	-0.12	-0.1	-0.11	-0.13	-0.13	-0.09	-0.11	-0.1	-0.11	-0.1	-0.11	-0.11	-0.11
Dec	Dec	Feb	Dec	Jan	Nov	Dec	Dec	Jan	Dec	Dec	Dec	Nov	Nov	Dec	Jan
0.289	0.26	0.319	0.212	0.242	0.184	0.275	0.259	0.314	0.213	0.205	0.189	0.195	0.195	0.275	0.242
May	Aug	Aug	Jul	Jul	Apr	Jun	Jul	Oct	Jun	Jun	May	May	Aug	Jun	Aug

Averag
20.99
Jan
31.2
May
0.009
Jan
0.023
Jun
-0.0004
Jul
0
Jan
99.57
Jul
102
Jan
-0.11
Nov
0.196
Jun
-0.11
Dec
0.231
Aug

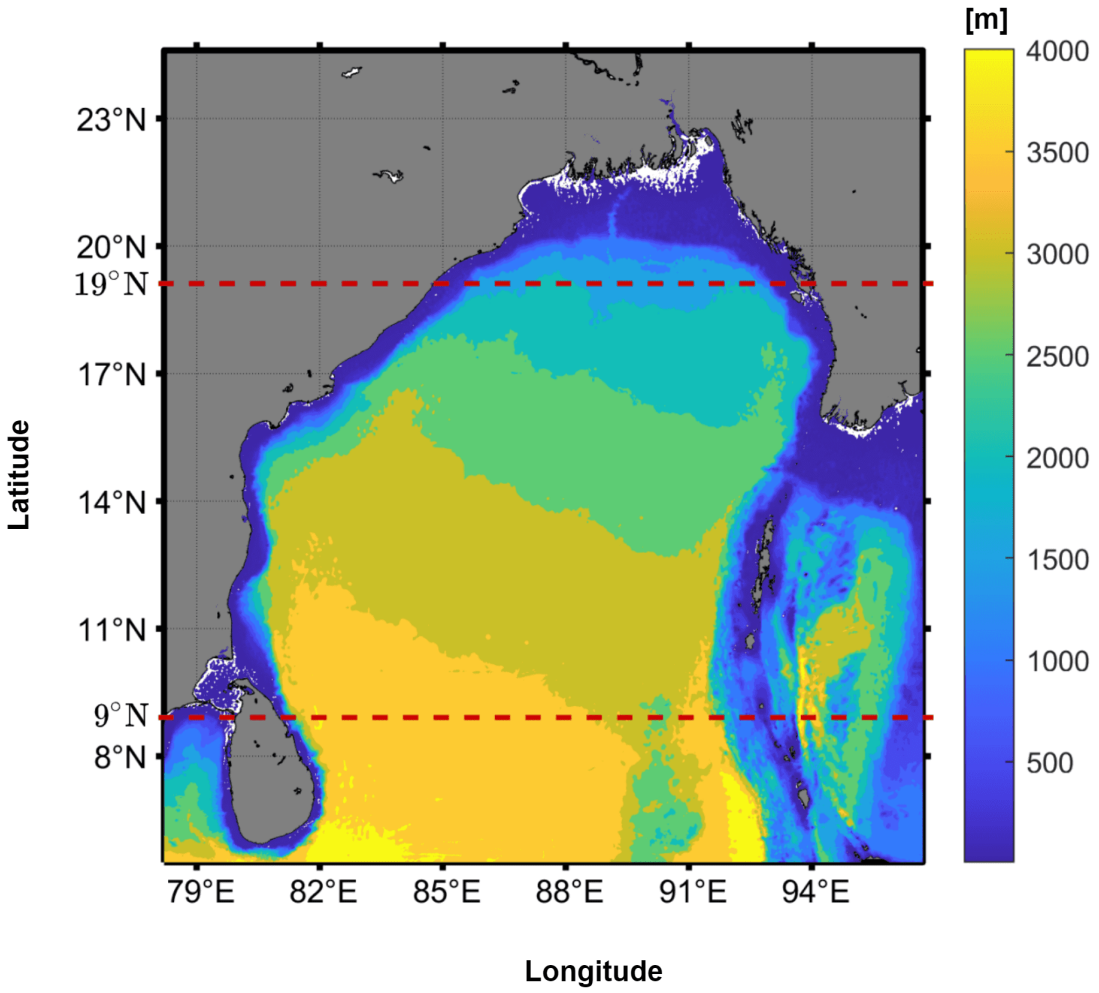

Fig. 1. BoB model domain bathymetry data, derived from SRTM15+ (https://topex.ucsd.edu/pub/archive/srtm15/V1/). Color gradations show different depths, ranging from yellow as a sign of the deepest depth to deep blue as the shallowest depth. While the gray color indicates land. The depth in the map is limited to 4000m.

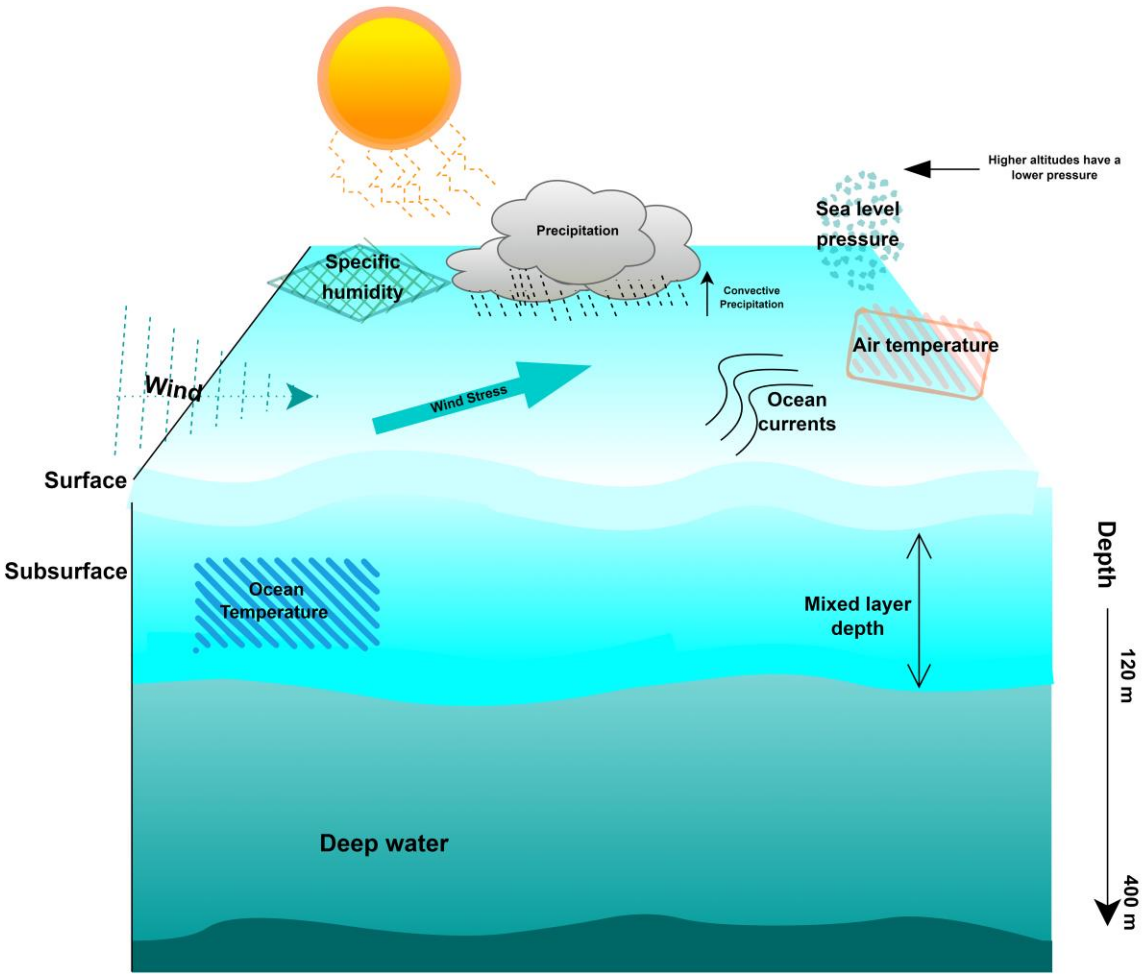

Fig. 2. A schematic diagram showing the interactions that occur at the air-sea interface involving meteorological parameters and mixed layer depth.

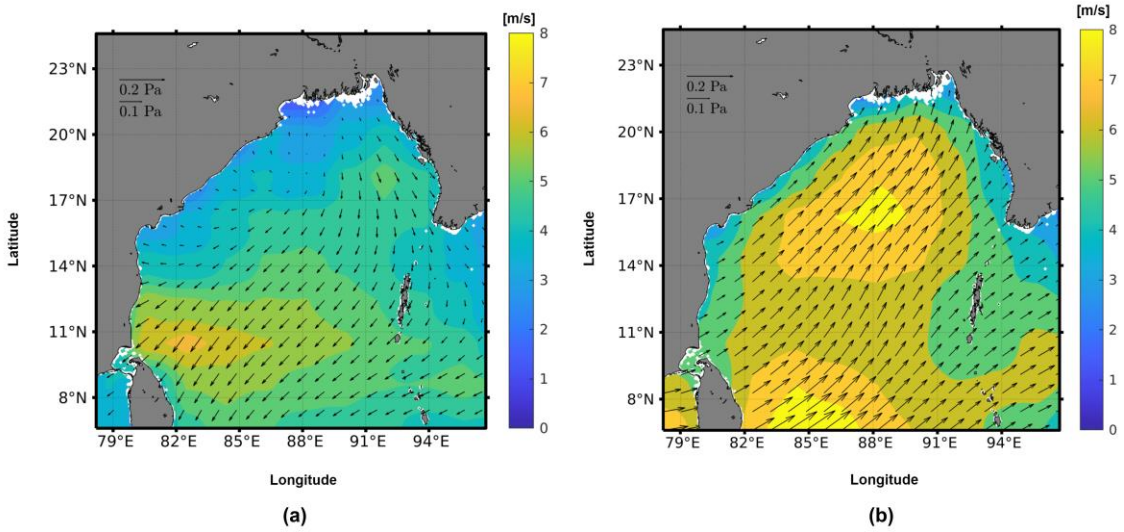

Fig. 3. The wind velocity (color in m/s) and wind stress (arrow in Pa) in (a) February and (b) August 2021, derived from NCEP/NCAR (https://psl.noaa.gov/data/gridded/data.ncep.reanalysis.html)

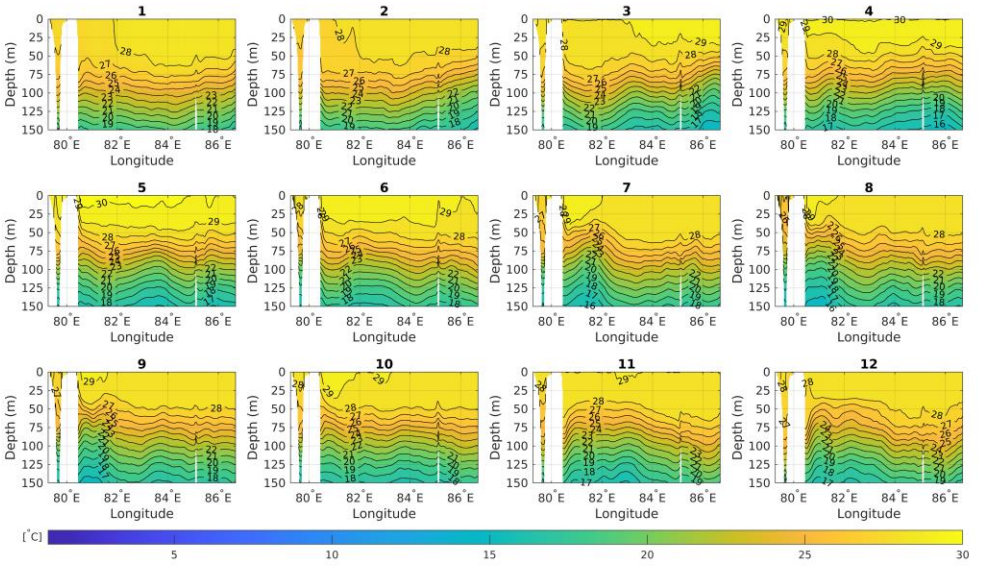

(a)

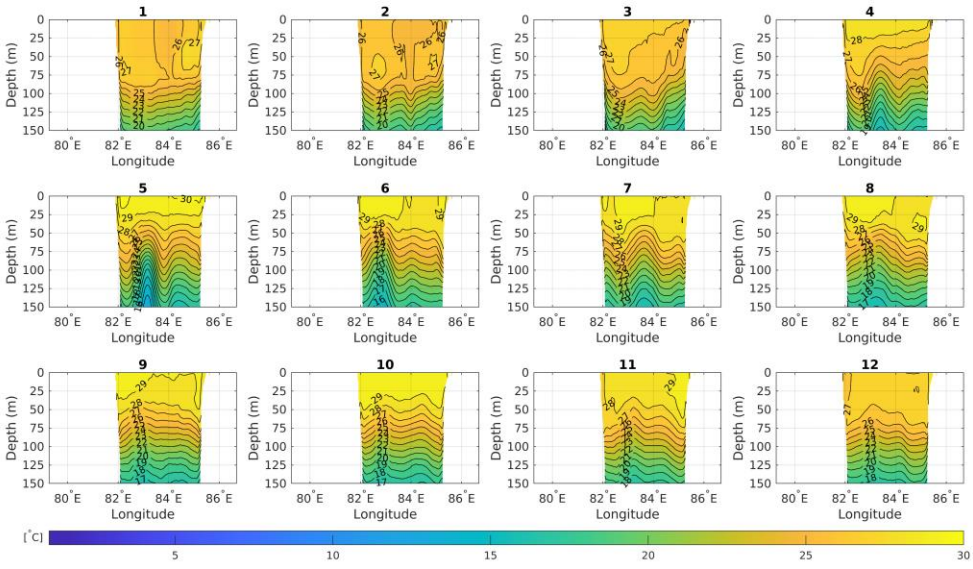

(b)

Fig. 4. The cross-section of the ocean temperature at (a) the latitude of 9º N and (b) the latitude of 19ºN in 2021 (12 months), derived from HYCOM (https://www.hycom.org/).

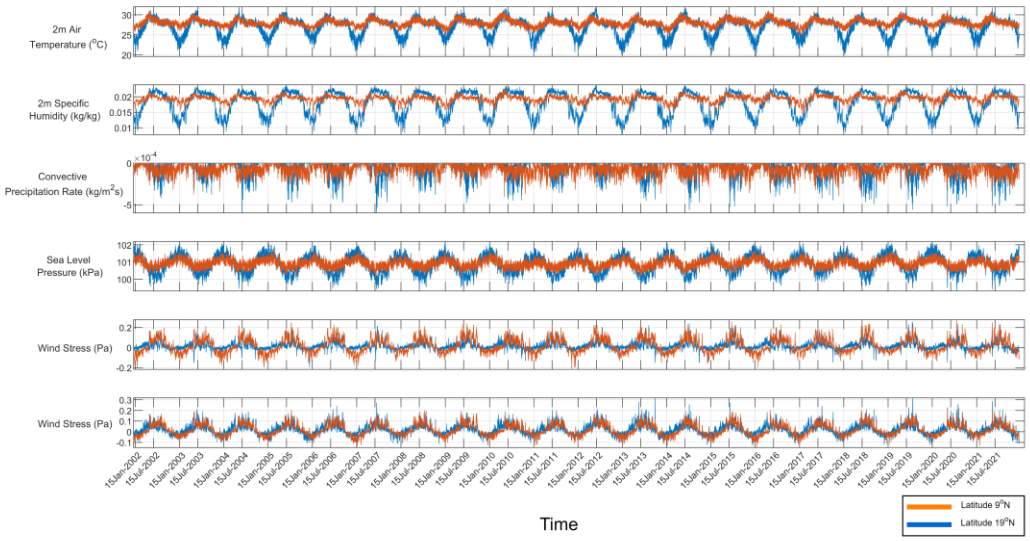

Fig. 5. Atmospheric forcing at the latitude of 9º N (orange color) and 19º N (blue color) from 2002 to 2021, derived from NCEP/NCAR (https://psl.noaa.gov/data/gridded/data.ncep.reanalysis.html).

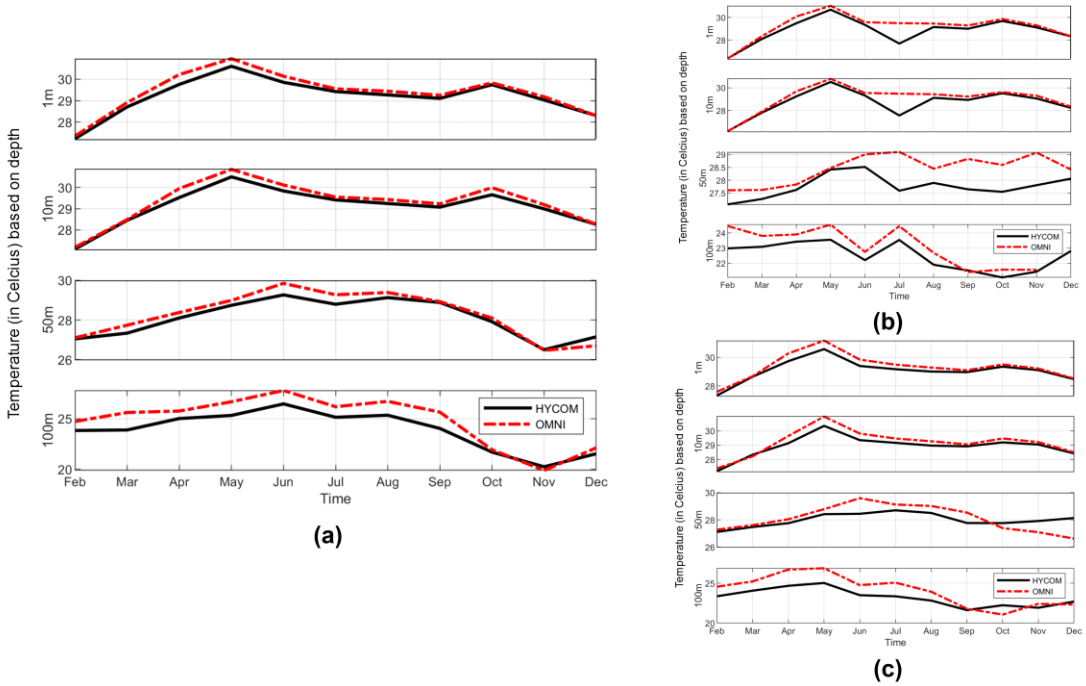

Fig. 6. Monthly average temperature data in February – December 2021, with (a) coordinate (84.17^{o}E,13.53^{o}N), (b) coordinate (87.99^{o}E,16.36^{o}N), and (c) coordinate (87^{o}E,13.99^{o}N).

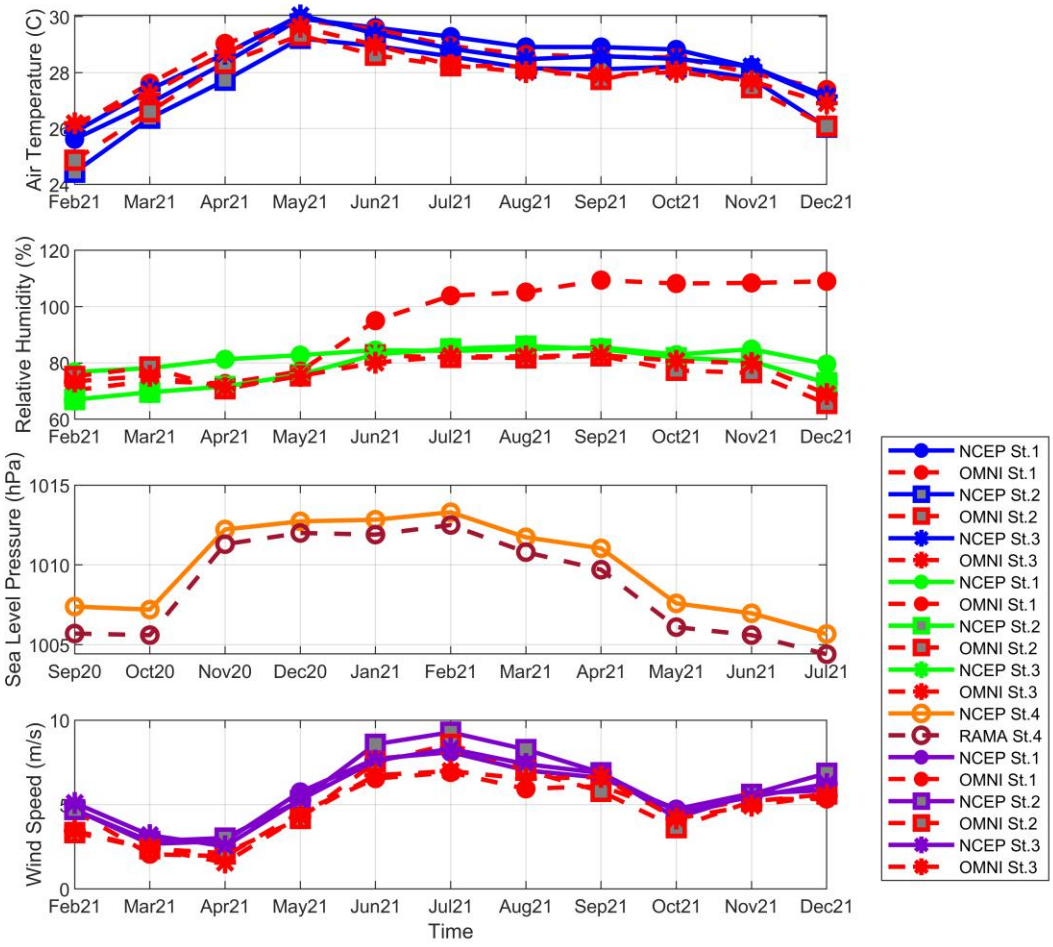

Fig. 7. Monthly average meteorology data in February – December 2021 with St. 1 as coordinate (84.17^{o}E,13.53^{o}N), St. 2 as coordinate (87.99^{o}E,16.36^{o}N), St. 3 as coordinate (87^{o}E,13.99^{o}N) and St. 4 as coordinate (90^{o}E,15^{o}N).

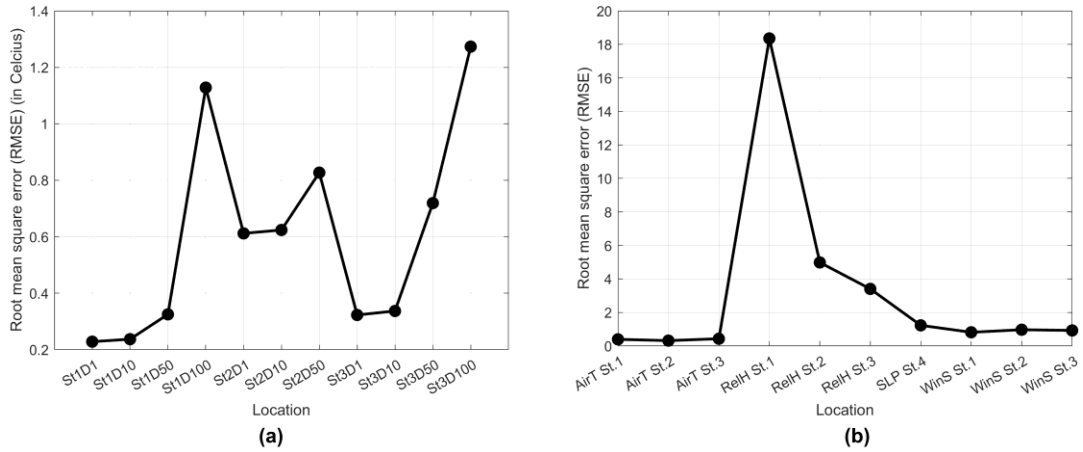

Fig. 8. Root mean square error (RMSE) for (a) Temperature data and (b) Meteorologi data based on location. Axis label in (a) representing Station 1-3 (coordinates (84.17^{o}E,13.53^{o}N), (87.99^{o}E,16.36^{o}N), (87^{o}E,13.99^{o}N)) based on depth 1m, 10m, 50m, and 100m. Meanwhile, the axis label in (b) represents parameters: AirT as Air Temperature, RelH as Relative Humidity, SLP as Sea Level Pressure, and WinS as Wind Speed based on location Station 1-4 (coordinates (84.17^{o}E,13.53^{o}N), (87.99^{o}E,16.36^{o}N), (87^{o}E,13.99^{o}N), (90^{o}E,15^{o}N)).

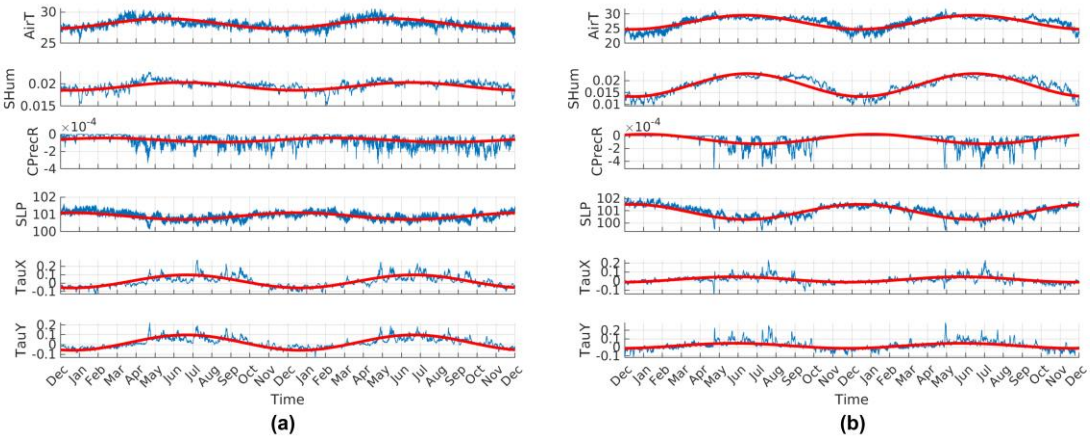

Fig. 9. Seasonal model for atmospheric forcing (a) at the latitude of 9^{o}N and (b) at the latitude of 19^{o}N, from 2020 to 2021.

Declaration of interests

☒ The authors declare that they have no known competing financial interests or personal relationships that could have appeared to influence the work reported in this paper.

☐The authors declare the following financial interests/personal relationships which may be considered as potential competing interests: